Electronic Supplementary Material (ESI) for Journal of Materials Chemistry

Supporting Information

Preparation of butadiene-styrene-vinyl pyridine rubber-graphene oxide hybrids through co-coagulation process and in situ interface tailoring

Zhenghai Tang,[a] Xiaohui Wu,[b] Baochun Guo,*[a,c] Liqun Zhang,*[b] and Demin Jia[a]

a Department of Polymer Materials and Engineering, South China University of Technology, Guangzhou 510640, China. E-mail: psbcguo@scut.edu.cn; Fax: +86 20 22236688; Tel: +86 20 87113374

b Key Laboratory of Beijing City for Preparation and Processing of Novel Polymer Materials, Beijing University of Chemical Technology, Beijing 100029, China. E-mail: zhanglq@mail.buct.edu.cn; Fax: +86 10 64421186; Tel: +86 10 64421186

c State Key Laboratory of Pulp and Paper Engineering, South China University of Technology, Guangzhou 510640, China

XRD patterns of HVPR/GO composites

As illustrated in Figure S1, all the composites displays the similar profile as that of the neat VPR, and the peak at 9.7° associated with GO (Figure1(d)) disappears. It indicates that the GO is well exfoliated in VPR matrix. The sharp peaks at 31.8° and 36.3° observed in all the curves can be assigned to the diffraction of zinc oxide.

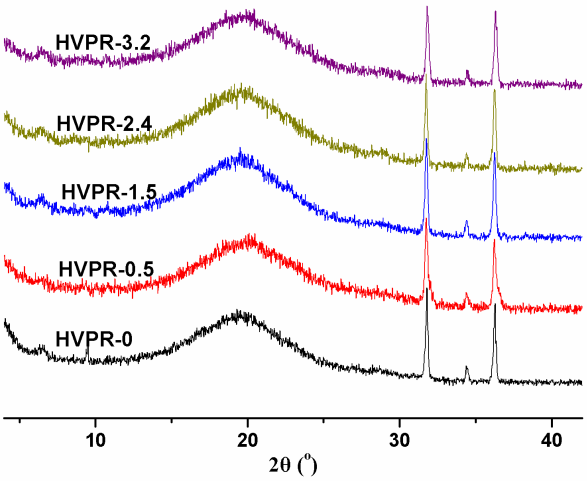

Fig. S1 XRD patterns of the neat VPR and HVPR/GO composites

TEM images of HVPR-3.6 and CaVPR-3.6

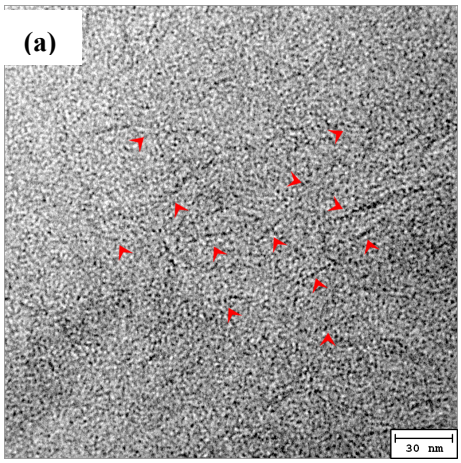

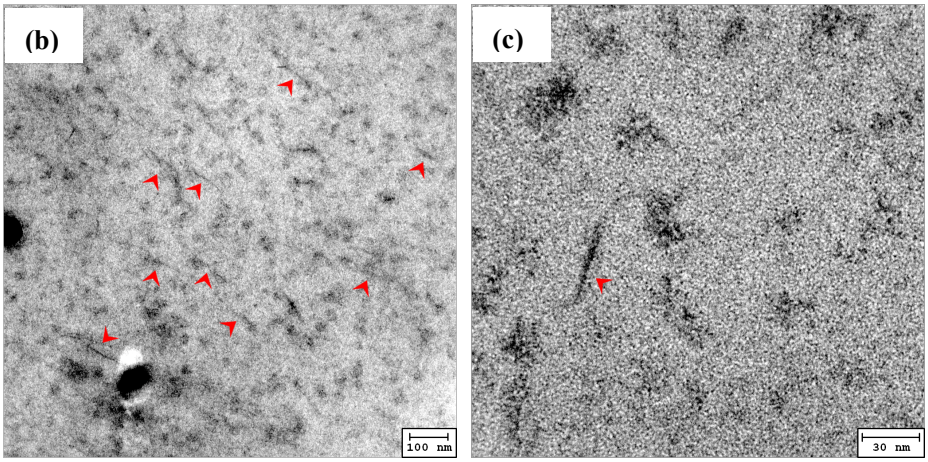

Fig. S2 TEM images of vulcanizated HVPR-3.6 (a), and CaVPR-3.6 (b),(c)

SAXS patterns of HVPR-3.6 and CaVPR-3.6

As seen in Fig. S3, HVPR-3.6 composite shows a broad peak with the interplanar spacing of ~4.3 nm. This is due to that the exfoliated GO sheets reassembled into GO mesostructure during vulcanization. This process is thermodynamically favored and facilitated by moulding pressure. It should be noted that only mesostructure of GO, instead of aggregates, is resulted in HVPR/GO system. In CaVPR/GO system, the much weak interfacial interaction cannot efficiently constrain the stacking of GO sheets. Consequently, the GO aggregation is found in CaVPR/GO system (Fig. S2). These observations can be intuitionistic verified by the TEM images. The GO restacking under pressure is similar to the inevitable stacking of clay sheets in rubber matrices under pressure or heating.[1-2]

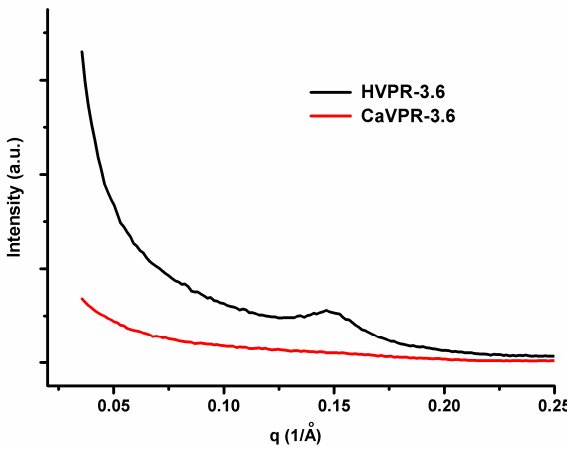

Fig. S3 SAXS patterns of HVPR-3.6 and CaVPR-3.6 composites

Size distribution of VPR latex, GO dispersion and VPR/GO mixture dispersion

Fig. S4 is the particle size measurement based on dynamic light scattering, the peak location of VPR latex is 97.3 nm, and the peak location of GO dispersion is 462 nm. It should be noted that measured sizes of GO is unable to reflect the actual sizes of GO sheets, because the measurement is based on the assumption that the particles are spherical.[3] Nevertheless, it provides a means of determining dispersion stability. In VPR/GO mixture dispersion, there are two peaks in the size distribution curves. One peak is suited at 97.3 nm, which is accordance with the size of VPR latex. The other peak at 669 nm is associated with the GO sheets. The size of GO in VPR/GO mixture is slightly larger than that in GO dispersion, which is due to that the VPR latex particles are absorbed onto GO sheets and thus the population of GO sheets is slightly larger. In addition, there are no aggregates are observed in the VPR/GO dispersion, indicating that the uniform dispersion of GO sheets and the stability of the VPR/GO dispersion.

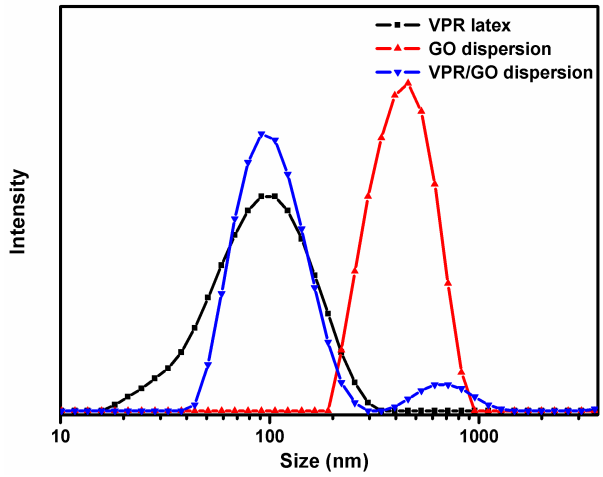

Fig. S4 Size distribution of VPR latex, GO dispersion and VPR/GO mixture dispersion with 2.4 vol% GO

Vulcanization curves of HVPR/GO and CaVPR/GO systems

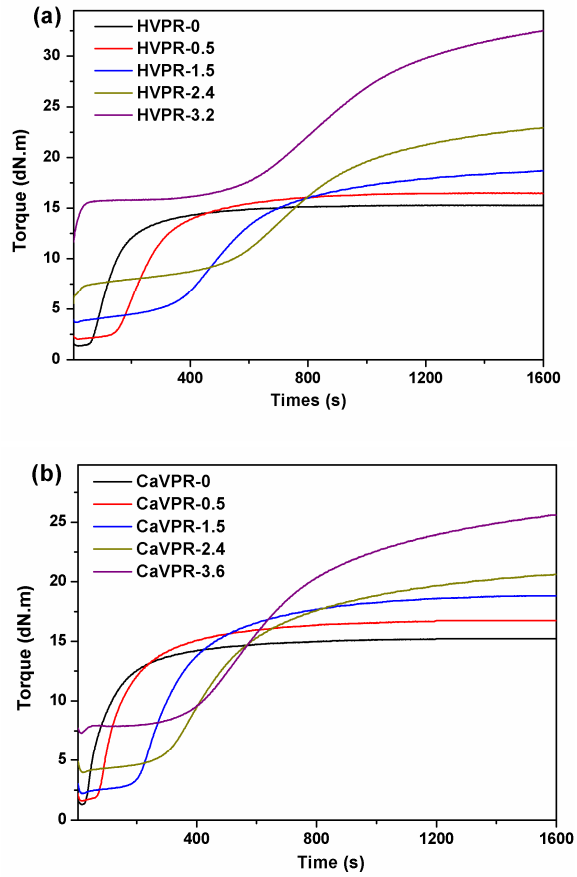

Fig. S5 Vulcanization curves of HVPR/GO and CaVPR/GO compounds

Comparison on the dynamic properties of HVPR-0.5 and CaVPR-0.5 composites

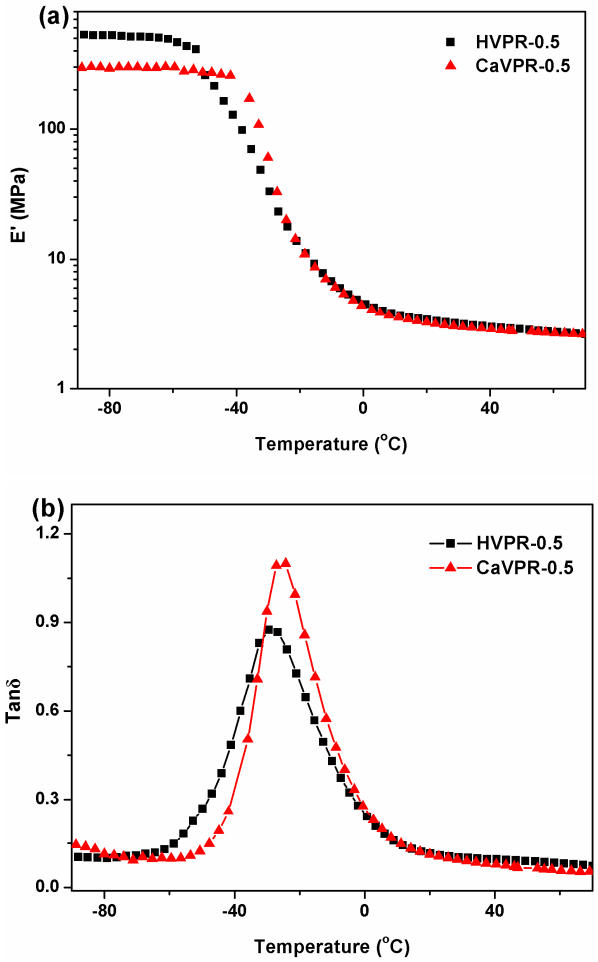

Fig. S6 Comparison on the dynamic properties of HVPR-0.5 and CaVPR-0.5 composites

Typical stress-strain curves of HVPR/GO and CaVPR/GO composites

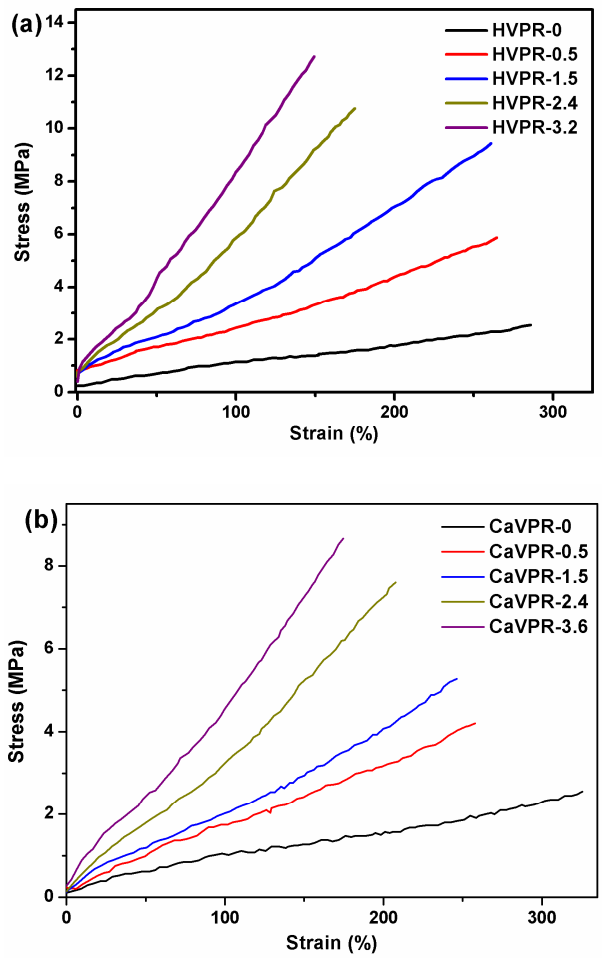

Fig. S7 Typical stress-strain curves of HVPR/GO (a), and CaVPR/GO composites (b)

Tab. S1 Comparison on mechanical enhancements in various composites or hybrids

Composites	Filler loading (%)	E' (by DMA) increase (%)	Tensile strength increase (%)	Modulus (by tensile test) increase (%)	Ref
GO/polycarbonate	3.0[a]	30[c]	N/A	N/A	4
GO/poly(methyl methacrylate)	4.0[a]	~52[c]	13	32	5
GO/ poly(ε-caprolactone)	10[a]	N/A	70	205	6
GO/carboxylated nitrile butadiene rubber	1.3[b]	N/A	-30	282	7
GO/poly(vinyl alcohol)	5.0[a]	N/A	46	194	8
Graphene/ polyacrylonitrile	4.0[a]	N/A	N/A	100	9
Graphene/polyurethane	2.0[a]	202[c]	239	N/A	10
Graphene/natural rubber	2.0[a]	40[c], 25[d]	47	72	11
MWNTs/poly(methyl methacrylate)	20[a]	1110[c]	N/A	N/A	12
MWNT-ZrP Nanoplatelets/Epoxy	0.4-4[a]	N/A	55	41	13
MWNT/polyimide	3.31[b]	N/A	46	44	14
Montmorillonite/natural rubber	10[a]	32[c]	131	191	15
Silicate layer/VPR	10[a]	N/A	277	360	16
HVPR-3.6	3.6 [b]	2145[c], 749[d]	350	644	present work

Note. (a) wt%, (b) vol%, (c) E' below Tg, and (d) above Tg

Tab. S2 Summary of the mechanical properties of HVPR/GO and CaVPR/GO composites

Sample	E' at -80°C (MPa)	E' at 30°C (MPa)	Stress at 100% strain (MPa)	Maximum stress (MPa)	Strain (%)	Shore A (Degree)
HVPR-0	184	2.37	1.14±0.08	2.73±0.27	290±7.2	51
CaVPR-0	N/A	N/A	1.02±0.04	2.54±0.13	307±13.3	51
HVPR-0.5	511	3.21	2.80±0.07	5.39±0.43	250±17.8	54
CaVPR-0.5	306	2.94	1.84±0.19	3.92±0.32	256±20.3	53
HVPR-1.5	726	6.14	3.83±0.39	9.26±0.21	234±16.8	61
CaVPR-1.5	N/A	N/A	1.93±0.09	5.16±0.33	242±19.0	59
HVPR-2.4	1330	9.28	6.77±0.31	10.81±0.71	164±11.6	70
CaVPR-2.4	N/A	N/A	3.03±0.14	7.42±0.28	212±8.9	64
HVPR-3.6	4130	20.13	8.52±0.34	12.28±0.61	157±5.7	75
CaVPR-3.6	N/A	N/A	4.50±0.25	9.69±0.77	203.8±15.1	66

Reference

(1) Liang, Y. R.; Lu, Y. L.; Wu, Y. P.; Ma, Y.; Zhang, L. Q., *Macromolecular Rapid Communications* **2005,** 26, (11), 926-931.

(2) Wang, X.; Huang, A.; Jia, D.; Li, Y., *European Polymer Journal* **2008,** 44, (9), 2784-2789.

(3) Li, D.; Muller, M. B.; Gilje, S.; Kaner, R. B.; Wallace, G. G., *Nature Nanotechnology* **2008,** 3, (2), 101-105.

(4) Potts, J. R.; Murali, S.; Zhu, Y.; Zhao, X.; Ruoff, R. S. *Macromolecules* **2011** 44, 6488.

(5) Potts, J. R.; Lee, S. H.; Alam, T. M.; An, J.; Stoller, M. D.; Piner, R. D.; Ruoff, R. S. *Carbon* **2011,** 49, 2615.

(6) Kai, W.; Hirota, Y.; Hua, L.; Inoue, Y. *J. Appl. Polym. Sci.* **2008,** 107, 1395.

(7) Bai, X.; Wan, C.; Zhang, Y.; Zhai, Y. *Carbon* **2011,** 49, 1608.

(8) Xu, Y. X.; Hong, W. J.; Bai, H.; Li, C.; Shi, G. Q. *Carbon* **2009,** 47, 3538.

(9) Mack, J. J.; Viculis, L. M.; Ali, A.; Luoh, R.; Yang, G.; Hahn, H. T.; Ko, F. K.; Kaner, R. B. *Adv. Mater.* **2005,** 17, 77.

(10) Wang, X.; Hu, Y. A.; Song, L.; Yang, H. Y.; Xing, W. Y.; Lu, H. D. *J.Mater. Chem.* **2011,** 21, 4222.

(11) Zhan, Y.; Wu, J.; Xia, H.; Yan, N.; Fei, G.; Yuan, G. *Macromol. Mater. Eng.***2011**, 296, 590.

(12) Hwang, G. L.; Shieh, Y. T.; Hwang, K. C. *Adv. Funct. Mater.* **2004**, 14, 487.

(13) Sun, D.; Chu, C. C.; Sue, H. J. *Chem. Mater.* **2010**, 22, 3773.

(14) Yuan, W.; Che, J.; Chan-Park, M. B. *Chem. Mater.***2011,** 23, 4149.

(15) Manchado, M.; Herrero, B.; Arroyo, M. *Polym. Int.* **2004**, 53, 1766.

(16) He, S.; Wang, Y.; Feng, Y.; Liu, Q.; Zhang, L. *Nanotechnology* **2010**, 21, 115601.